Resilient Microgrid Scheduling Considering Multi-Level Load Priorities

Guodong Liu*, Madhu S. Chinthavali*, Nils Stenvig*, Xue Li†, Tao Jiang†, Yichen Zhang‡ and Kevin Tomsovic‡
*Oak Ridge National Laboratory, Oak Ridge, TN 37381
Email: liug@ornl.gov, chinthavalim@ornl.gov, stenvignm@ornl.gov
†Department of Electrical Engineering, Northeast Electric Power University, Jilin, China 132012
Email: xli@neepu.edu.cn, tjiang@neepu.edu.cn
‡Department of Electrical Engineering and Computer Science, University of Tennessee, Knoxville, TN 37996
Email: yzhan124@utk.edu, tomsovic@tennessee.edu

***Abstract*—In this paper, we propose a novel resilient microgrid scheduling model considering the multi-level load priorities. The resiliency of the microgrid is guaranteed by quickly adjusting the output of committed local resources and shedding the loads with low priorities when the power supply from the main grid is interrupted. Considering the uncertainty of renewable energy resources and loads as well as exchanged power at PCC, the probability of successful islanding (PSI) is used to quantify the resiliency of electricity supply for various loads with different priorities. Then, the multi-level priorities are enforced through chance constrains. Results of numerical simulation validate the proposed resilient scheduling model. In addition, the impacts of resiliency requirement of loads with high priority on the resiliency of loads with low priority are analyzed as well.**

***Index Terms*—Microgrid, resilient scheduling, probability of successful islanding, load priority, chance constraints.**

NOMENCLATURE

The symbols used in this paper are defined below. A $\triangle$ indicates forecast error while $\hat{}$ indicates the forecast value.

A. Indices

i	Index of dispatchable units, running from 1 to N_G.
d	Index of loads with priority level I, II and III, running from 1 to N_D^{I}, N_D^{II} and N_D^{III}.
b	Index of batteries, running from 1 to N_B.
t	Index of time periods, running from 1 to N_T.
m	Index of energy blocks offered by generators, running from 1 to N_I.

This manuscript has been authored by UT-Battelle, LLC under Contract No. DE-AC05-00OR22725 with the U.S. Department of Energy. The United States Government retains and the publisher, by accepting the article for publication, acknowledges that the United States Government retains a non-exclusive, paid-up, irrevocable, world-wide license to publish or reproduce the published form of this manuscript, or allow others to do so, for United States Government purposes. The Department of Energy will provide public access to these results of federally sponsored research in accordance with the DOE Public Access Plan(http://energy.gov/downloads/doe-public-access-plan).

This work also made use of Engineering Research Center Shared Facilities supported by the Engineering Research Center Program of the National Science Foundation and the Department of Energy under NSF Award Number EEC-1041877 and the CURENT Industry Partnership Program.

B. Variables

1) Binary Variables:

u_{it}	1 if unit i is scheduled on during period t and 0 otherwise.
u_{bt}^{C}	1 if battery b is scheduled charging during period t and 0 otherwise.
u_{bt}^{D}	1 if battery b is scheduled discharging during period t and 0 otherwise.

2) Continuous Variables:

$p_{it}\,(m)$	Power output scheduled from the m-th block of energy offer by dispatchable unit i during period t . Limited to $p_{it}^{max}\,(m)$.
P_{it}	Power output scheduled from dispatchable unit i during period t.
P_t^{PCC}	Exchanged power at PCC during period t.
$P_{bt}^{\mathrm{C}}, P_{bt}^{\mathrm{D}}$	Charging/discharging power of battery b during period t.
P_{bt}	Output power of battery b during period t.
SOC_{bt}	State of charge of battery b during period t.
R_{it}^{U}, R_{it}^{D}	Up- and down-spinning reserve of unit i during period t.
R_{bt}^{U}, R_{bt}^{D}	Up- and down-spinning reserve of battery b during period t.
$\mathrm{PSI}_t^{\mathrm{I}}, \mathrm{PSI}_t^{\mathrm{II}}, \mathrm{PSI}_t^{\mathrm{III}}$	PSI of loads with level I, II and III priority during period t.
α_{dt}^{I}, $\alpha_{dt}^{\mathrm{II}}$	Percentage of potentionally shedding load d with level I or II priority during period t.

C. Constants

$\lambda_{it}\,(m)$	Marginal cost of the m-th block of energy offer by dispatchable unit i during period t.
C_{bt}	Degradation cost of battery b during period t.
λ_t^{PCC}	Purchasing/selling price of energy from/to distribution grid during period t.
A_i	Operating cost of unit i at the point of $P_i^{\min}$.
Q_{it}^{U}, Q_{it}^{D}	Cost of up- and down-spinning reserve of unit i during period t.
Q_{bt}^{U}, Q_{bt}^{D}	Cost of up- and down-spinning reserve of battery b during period t.

Q_{dt}^{I}, Q_{dt}^{II} Cost of potentially shedding load d with level I or II priority during period t.
$P_i^{\max}, P_i^{\min}$ Maximum/minimum output of DG i.
P_t^{W} Wind turbine power output during period t.
P_t^{PV} PV power output during period t.
$P_{dt}^{\mathrm{I}}, P_{dt}^{\mathrm{II}}, P_{dt}^{\mathrm{III}}$ Power consumption scheduled for load d with with level I, II and III priority during period t.
$\triangle N_t^D$ Net demand forecast error during period t.
μ_t, σ_t Mean and standard deviation of $\triangle N_t^D$.
$\mathrm{PSI}^{\mathrm{I,req}}, \mathrm{PSI}^{\mathrm{II,req}}, \mathrm{PSI}^{\mathrm{III,req}}$ PSI requirements of loads with level I, II and III priority.
$P_b^{\mathrm{C,max}}, P_b^{\mathrm{D,max}}$ Maximum charging/discharging power of battery b.
$SOC_{bt}^{\max}, SOC_{bt}^{\min}$ Maximum/minimum state of charge of battery b during period t.
$\eta_b^{\mathrm{C}}, \eta_b^D$ Battery charging/discharging efficiency factor.
$\triangle t$ Time duration of each period.
τ Amount of time available of DGs and batteries to ramp up/down their output to deliver the reserve.

I. Introduction

A microgrid can be defined as a low voltage distribution network comprising various distributed generators (DGs), energy storage systems (ESSs), and responsive loads [1]. It is connected to the main distribution network at the Point of Common Coupling (PCC), importing or exporting power to the distribution network. In particular, a microgrid has the ability to intentionally disconnect from the main grid (e.g., during disturbances of utilities) and continue to supply all or selected loads in its own islanded portion without any interruption [2]. By virtue of this feature, microgrids could enhance the resiliency of the power system through lowing the probability and amount of load shedding, preventing cascading blackouts and accelerating the restoration [3]. With these benefits, more and more microgrids have been deployed in recent years [4].

Resilience is the ability of power systems to prepare for and adapt to low-probability high-impact incidents and withstand and recover rapidly from disruptions. Considerable efforts have been devoted to scheduling of microgrids with resiliency considerations in recent years. In [5], the adequacy constraints are considered in the economic dispatch model of a microgrid to ensure seamless transition from interconnected to autonomous operation of the microgrid could be achieved. Considering the uncertainty of renewable generation and demand, a probabilistic chance constraint is proposed to guarantee that the microgrid is capable to meeting the local demand with specified probability in [6]. In [7], a methodology to quantify the spinning reserve of a microgrid based on the optimal tradeoff between reliability and economics is proposed. A stochastic microgrid scheduling model with chance-constrained islanding capability to ensure successful islanding of a microgrid with a specified probability is proposed in [8]. Robust optimization-based scheduling model for microgrid operation with reserve requirements is proposed in [9]. A resiliency-oriented microgrid optimal scheduling model considering the main grid supply interruption time and duration was proposed in [10]. The model was extended to consider the uncertainties of renewable generation and load in [11].

In the existing literature, research studies on resilient microgrid scheduling have been mostly focused on the dispatch of DGs and ESSs to satisfy certain security margins enforced by resiliency requirements. The demand response has been rarely considered or simply modeled as critical load and non-critical load. Similar to DGs and ESS, the non-critical loads provide additional security margins through voluntary load shedding. By this way, the resiliency of critical loads is guaranteed. However, the resiliency of non-critical loads has been ignored completely. In fact, the non-critical loads in a microgrid might also have certain resiliency requirement, which is normally lower than that of critical loads. More generally, a microgrid might have multi-level load priorities. Each level of load priority has corresponding resiliency requirements. In the extreme case, each load in the microgrid could specify its own resiliency requirements. Therefore, designing a resilient microgrid scheduling model which could satisfy the resiliency requirements of multi-level load priorities is necessary.

In view of the shortcomings of the existing microgrid scheduling strategies, a new resilient microgrid scheduling model considering the multi-level load priorities is developed in this paper. The probability of successful islanding (PSI) proposed in [8] is used as a resiliency index to indicate the probability that a microgrid is maintaining adequate security margin to meet local demand and accommodate local renewable generation after islanding. We extend the microgrid scheduling model in [8] to ensure the resiliency requirements of multi-level load priorities. The PSI requirement of each priority level is explicitly specified through a chance constraint. The main contributions of this paper are as follows:

1) Proposed a new resilient microgrid scheduling model considering the user specified multi-level load priorities;
2) Validated the effectiveness and accuracy of the proposed resilient microgrid scheduling model; and
3) Analyzed the impact of resiliency of loads with high priority on the resiliency of loads with low priority.

The rest of this paper is organized as follows. In Section II, the resilient microgrid scheduling model with multi-level load priorities is presented. Results of case studies are presented in Section III. Finally, Section IV concludes the paper.

II. Resilient Microgrid Scheduling with Multi-Level Load Priorities

A. Component Models

The microgrid considered in this paper consists of dispatchable and undispatchable generation, energy storage facilities and various loads with different priorities. Dispatchable generation (e.g., diesel generators, microturbines and fuel cells) could be controlled by a microgrid master controller to provide both power and reserve, while undispatchable generation (e.g., wind turbines and PV panels) have uncertain power output depending on the meteorological conditions of wind speed, temperature and solar irradiance. For simplicity, we assume

both wind and PV power forecast errors are modeled as independent normally distributed random variables [6]. The load forecast error is assumed to follow normal distribution and be independent of renewable generation [7]. Three levels of priority are assumed for loads. Level I indicates lowest priority, level II indicates medium priority and level III indicates highest priority. Nevertheless, more priority levels could be added. Shedding loads with lower priorities is taken as the last resort to enforce the resiliency of loads with higher priorities.

B. Problem Formulation

This subsection describes the optimization model of the proposed resilient microgrid scheduling with multi-level load priorities. In the context of a microgrid with dispatchable and undispatchable generation as well as ESSs (e.g., batteries) integration, the objective aims at minimizing the total operation cost, including generation cost and spinning reserve cost of local resources as well as purchasing cost of energy form main grid. The objective function is shown in (1). Specifically, the first and second line are the fuel cost of DGs (including start-up cost); the third line is the energy purchasing/selling cost/benefit from distribution grid and the battery degradation cost; the fourth and fifth lines are cost of up- and down-spinning reserve from both DGs and ESSs; the sixth line are the costs of potential load interruptions.

$$\begin{aligned}\min \quad & \sum_{t=1}^{N_T}\sum_{i=1}^{N_G}\left[\sum_{m=1}^{N_I}\lambda_{it}(m)p_{it}(m)+A_i u_{it}\right] \\ & +\sum_{t=1}^{N_T}\sum_{i=1}^{N_G} SU_{it}\left(u_{it},u_{i,t-1}\right) \\ & +\sum_{t=1}^{N_T}\lambda_t^{\mathrm{PCC}}P_t^{\mathrm{PCC}}+\sum_{t=1}^{N_T}\sum_{b=1}^{N_B}C_{bt}\left(P_{bt}^{\mathrm{C}}+P_{bt}^{\mathrm{D}}\right) \\ & +\sum_{t=1}^{N_T}\sum_{i=1}^{N_G}\left(Q_{it}^{\mathrm{U}}R_{it}^{\mathrm{U}}+Q_{it}^{\mathrm{D}}R_{it}^{\mathrm{D}}\right) \\ & +\sum_{t=1}^{N_T}\sum_{b=1}^{N_B}\left(Q_{bt}^{\mathrm{U}}R_{bt}^{\mathrm{U}}+Q_{bt}^{\mathrm{D}}R_{bt}^{\mathrm{D}}\right) \\ & +\sum_{t=1}^{N_T}\sum_{d=1}^{N_D^{\mathrm{I}}}\alpha_{dt}^{\mathrm{I}}\hat{P_{dt}^{\mathrm{I}}}Q_{dt}^{\mathrm{I}}+\sum_{t=1}^{N_T}\sum_{d=1}^{N_D^{\mathrm{II}}}\alpha_{dt}^{\mathrm{II}}\hat{P_{dt}^{\mathrm{II}}}Q_{dt}^{\mathrm{II}} \end{aligned} \tag{1}$$

The objective is subject to the following constraints:

$$P_{it}=\sum_{m=1}^{N_I}p_{it}(m)+u_{it}P_i^{\min} \quad \forall i,\forall t \tag{2}$$

$$0\le p_{it}(m)\le p_{it}^{\max}(m) \quad \forall i,\forall t,\forall m \tag{3}$$

$$P_i^{\min}u_{it}\le P_{it}\le P_i^{\max}u_{it} \quad \forall i,\forall t \tag{4}$$

$$R_{it}^{\mathrm{U}}\le P_i^{\max}u_{it}-P_{it} \quad \forall i,\forall t \tag{5}$$

$$R_{it}^{\mathrm{U}}\le u_{it}R_i^{\mathrm{U,max}}\tau \quad \forall i,\forall t \tag{6}$$

$$R_{it}^{\mathrm{D}}\le P_{it}-P_i^{\min}u_{it} \quad \forall i,\forall t \tag{7}$$

$$R_{it}^{\mathrm{D}}\le u_{it}R_i^{\mathrm{D,max}}\tau \quad \forall i,\forall t \tag{8}$$

$$0\le P_{bt}^{\mathrm{C}}\le P_b^{\mathrm{C,max}}u_{bt}^{\mathrm{C}} \quad \forall b,\forall t \tag{9}$$

$$0\le P_{bt}^{\mathrm{D}}\le P_b^{\mathrm{D,max}}u_{bt}^{\mathrm{D}} \quad \forall b,\forall t \tag{10}$$

$$u_{bt}^{\mathrm{C}}+u_{bt}^{\mathrm{D}}\le 1 \quad \forall b,\forall t \tag{11}$$

$$SOC_{bt}=SOC_{b,t-1}+P_{bt}^{\mathrm{C}}\eta_b^{\mathrm{C}}\triangle t-P_{bt}^{\mathrm{D}}\frac{1}{\eta_b^{\mathrm{D}}}\triangle t \quad \forall b,\forall t \tag{12}$$

$$SOC_{bt}^{\min}\le SOC_{bt}\le SOC_{bt}^{\max} \quad \forall b,\forall t \tag{13}$$

$$P_{bt}=P_{bt}^{\mathrm{D}}-P_{bt}^{\mathrm{C}} \quad \forall b,\forall t \tag{14}$$

$$R_{bt}^{\mathrm{U}}\le P_b^{\mathrm{D,max}}-P_{bt} \quad \forall b,\forall t \tag{15}$$

$$R_{bt}^{\mathrm{U}}\le \eta_b^{\mathrm{D}}\left(SOC_{bt}-SOC_{bt}^{\min}\right)/\tau \quad \forall b,\forall t \tag{16}$$

$$R_{bt}^{\mathrm{D}}\le P_b^{\mathrm{C,max}}+P_{bt} \quad \forall b,\forall t \tag{17}$$

$$R_{bt}^{\mathrm{D}}\le 1/\eta_b^{\mathrm{C}}\left(SOC_{bt}^{\max}-SOC_{bt}\right)/\tau \quad \forall b,\forall t \tag{18}$$

$$\begin{aligned}&\textstyle\sum_{i=1}^{N_G}P_{it}+\hat{P_t^{\mathrm{W}}}+\hat{P_t^{\mathrm{PV}}}+P_t^{\mathrm{PCC}}+\sum_{b=1}^{N_B}\left(P_{bt}^{\mathrm{D}}-P_{bt}^{\mathrm{C}}\right) \\ &\quad=\textstyle\sum_{d=1}^{N_D^{\mathrm{I}}}\hat{P_{dt}^{\mathrm{I}}}+\sum_{d=1}^{N_D^{\mathrm{II}}}\hat{P_{dt}^{\mathrm{II}}}+\sum_{d=1}^{N_D^{\mathrm{III}}}\hat{P_{dt}^{\mathrm{III}}} \quad \forall t\end{aligned} \tag{19}$$

$$\triangle N_t^D=\sum_{d=1}^{N_D^{\mathrm{I}}}\triangle P_{dt}^{\mathrm{I}}+\sum_{d=1}^{N_D^{\mathrm{II}}}\triangle P_{dt}^{\mathrm{II}}+\sum_{d=1}^{N_D^{\mathrm{III}}}\triangle P_{dt}^{\mathrm{III}}-\triangle P_t^{\mathrm{W}}-\triangle P_t^{\mathrm{PV}} \tag{20}$$

For DGs, constraints (2) and (3) approximate the production cost of dispatchable generators by blocks. Constraint (4) forces the output of DG to be zero if it is not committed. The up-spinning reserve of DG is limited by the difference between its maximum capacity and current output in (5) and its ramping rate in (6). Similarly, the down-spinning reserve constraints are included in (7) and (8). For ESSs, constraints (9) and (10) are the maximum charging/discharging power of an ESS. These two states are mutually exclusive, which is ensured by (11). The ESS state of charge (SOC) is defined by (12) and the limit of SOC is enforced by (13). The output power of an ESS is represented in (14). Similar to DGs, the up-spinning reserve of an ESS is constrained by the difference between its current SOC and minimum SOC in (15) and the difference between its maximum discharging power and current output in (16). The down-spinning reserve constraints of an ESS are included as in (17) and (18). The generation and demand balance of the microgrid is enforced by (19). The net demand forecast error $\triangle N_t^D$ is defined in (20). As mentioned earlier, we assume both wind and PV power forecast error as well as load forecast error are modeled as independent normal distributed random variables. Thus, $\triangle N_t^D$ also follows normal distribution.

The resiliency requirement of loads with level I priority is enforced by constraint (21), which guarantees the probability of the microgrid maintaining adequate up- and down-spinning reserve to continuously satisfy all loads with priorities equal or higher than level I after instantaneously islanding is no less than $\mathrm{PSI}^{\mathrm{I,req}}$. Similarly, the resiliency requirement of loads with level II priority is enforced by constraint (22), which guarantees the probability of continuously satisfying all loads with priorities equal or higher than level II after instantaneously islanding is no less than $\mathrm{PSI}^{\mathrm{II,req}}$. Note that certain percentage of level I loads is allowed to be shed as the last resort to ensure supply of loads with priorities equal or higher than level II. The resiliency requirement of loads with the highest priority, i.e., level III, is enforced by constraint

$$\mathrm{PSI}_t^{\mathrm{I}} = \mathrm{P}\left(-\sum_{i=1}^{N_G} R_{it}^{\mathrm{D}} - \sum_{b=1}^{N_B} R_{bt}^{\mathrm{D}} \le P_t^{\mathrm{PCC}} + \triangle N_t^D \le \sum_{i=1}^{N_G} R_{it}^{\mathrm{U}} + \sum_{b=1}^{N_B} R_{bt}^{\mathrm{U}} \right) \le \mathrm{PSI}^{\mathrm{I,req}} \tag{21}$$

$$\mathrm{PSI}_t^{\mathrm{II}} = \mathrm{P}\left(-\sum_{i=1}^{N_G} R_{it}^{\mathrm{D}} - \sum_{b=1}^{N_B} R_{bt}^{\mathrm{D}} \le P_t^{\mathrm{PCC}} + \triangle N_t^D \le \sum_{i=1}^{N_G} R_{it}^{\mathrm{U}} + \sum_{b=1}^{N_B} R_{bt}^{\mathrm{U}} + \sum_{d=1}^{N_D^{\mathrm{I}}} \alpha_{dt}^{\mathrm{I}} \hat{P}_{dt}^{\mathrm{I}} \right) \le \mathrm{PSI}^{\mathrm{II,req}} \tag{22}$$

$$\mathrm{PSI}_t^{\mathrm{III}} = \mathrm{P}\left(-\sum_{i=1}^{N_G} R_{it}^{\mathrm{D}} - \sum_{b=1}^{N_B} R_{bt}^{\mathrm{D}} \le P_t^{\mathrm{PCC}} + \triangle N_t^D \le \sum_{i=1}^{N_G} R_{it}^{\mathrm{U}} + \sum_{b=1}^{N_B} R_{bt}^{\mathrm{U}} + \sum_{d=1}^{N_D^{\mathrm{I}}} \hat{P}_{dt}^{\mathrm{I}} + \sum_{d=1}^{N_D^{\mathrm{II}}} \alpha_{dt}^{\mathrm{II}} \hat{P}_{dt}^{\mathrm{II}} \right) \le \mathrm{PSI}^{\mathrm{III,req}} \tag{23}$$

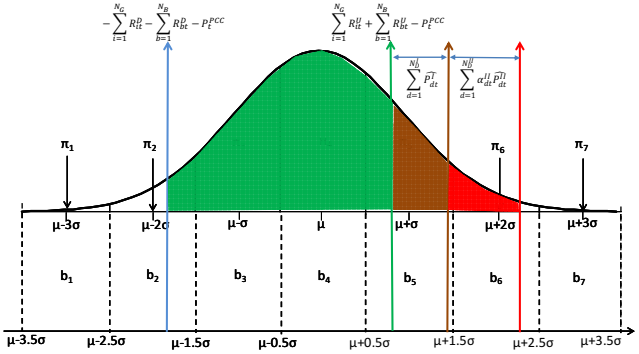

Fig. 1: Illustration of PSI of loads with level III priority

(23), which allows all level I loads and certain percentage of level II loads being shed.

A graphical illustration of PSI of loads with level III priority is shown in Fig. 1. The net demand forecast error $\triangle N_t^D$ follows normal distribution. The green area indicates the PSI of microgrid without load shedding, i.e., $\mathrm{PSI}_t^{\mathrm{I}}$. The brown area indicates additional PSI by shedding of loads with level I priority. Furthermore, additional PSI, i.e., the red area is acquired by shedding of loads with level II priority. Therefore, the PSI of loads with level III priority is the sum of the green area, the brown area and the red area. Based on the approximation method proposed in [8], the PSI index in (21)-(23) are reformulated into mixed integer linear format. Thus, the proposed resilient scheduling model could be solved by mixed integer linear programming (MILP). Note that the proposed model explicitly guarantees the resiliency requirements of loads with multi-level priorities.

III. Case Studies

The proposed resilient microgrid scheduling model with multi-level load priorities is demonstrated on the modified ORNL Distributed Energy Control and Communication (DECC) lab microgrid test system [8]. All parameters for the dispatchable generators, forecast wind power, PV power and loads as well as the day-ahead market price can be found in [8]. The forecast errors of wind power and PV power are assumed to be Gaussian distribution with zero mean and 15% of standard deviation. The load forecast errors are assumed to be Gaussian distribution with zero mean and 3% of standard deviation. All loads are divided into two groups based on their priorities. Loads with level I priority account for 30% of the total demand, while loads with level II priority account for the rest 70%. The analysis is conducted for a 24-hour scheduling horizon and each time interval is set to be one hour. All numerical simulations are coded in MATLAB and solved using the MILP solver CPLEX 12.2. With a pre-specified duality gap of 0.1%, the running time of each case is less than 10 seconds on a 2.66 GHz Windows-based PC with 4 G bytes of RAM.

A. Validate the Effectiveness of the Proposed Resilient Microgrid Scheduling Model

To validate the solution of the proposed resilient microgrid scheduling model with multi-level load priorities, Monte-Carlo simulation is used to generate 5,000 scenarios of renewable generation and loads. Both wind and PV power forecast errors as well as load forecast errors are modeled as independent normal distributed random variables with zero mean. For each scenario, the inequalities in parentheses in constraints (21)-(23) are tested, separately. If the inequality in parentheses is satisfied, this scenario is counted as capable of successful islanding for the corresponding level of priority. By this way, the $\mathrm{PSI}^{\mathrm{II}}$ under different $\mathrm{PSI}^{\mathrm{I}}$ and $\mathrm{PSI}^{\mathrm{II}}$ settings are calculated and shown in Fig. 2. As observed, the calculated values of $\mathrm{PSI}^{\mathrm{II}}$ are very close to the corresponding $\mathrm{PSI}^{\mathrm{II}}$ settings.

In order to show the impacts of resiliency requirement of loads with high priority on the resiliency of loads with low priority, the $\mathrm{PSI}^{\mathrm{I}}$ under different $\mathrm{PSI}^{\mathrm{II}}$ settings are calculated and shown in Fig. 3. As can be seen, the actual PSI of loads with level I priority are obviously affected by the PSI settings of loads with level II priority. For certain time intervals, e.g., hour 11-13, the calculated values of $\mathrm{PSI}^{\mathrm{I}}$ are almost the same as those of $\mathrm{PSI}^{\mathrm{II}}$. This situation happens when $\sum_{i=1}^{N_G} R_{it}^{\mathrm{U}} + \sum_{b=1}^{N_B} R_{bt}^{\mathrm{U}} - P_t^{\mathrm{PCC}}$ is relatively large, i.e., the green axis is located at the right tail of normal distribution. Under this condition, shedding of loads with lower priority has relatively limited influence on the PSI of loads with higher priority. Thus, the calculated values of $\mathrm{PSI}^{\mathrm{I}}$ and $\mathrm{PSI}^{\mathrm{II}}$ are very close. Nevertheless, the $\mathrm{PSI}^{\mathrm{I,req}}$ of level I loads are still satisfied for all time intervals.

B. Comparing Total Cost Under Different PSI Settings

The total operating costs of the microgrid with different levels of $\mathrm{PSI}^{\mathrm{I}}$ and $\mathrm{PSI}^{\mathrm{II}}$ settings are compared in Fig. 4. Generally, with increasing $\mathrm{PSI}^{\mathrm{I,req}}$ and $\mathrm{PSI}^{\mathrm{II,req}}$, the total operating cost of the microgrid monotonically increases but in a highly nonlinear fashion. For example, a small increase

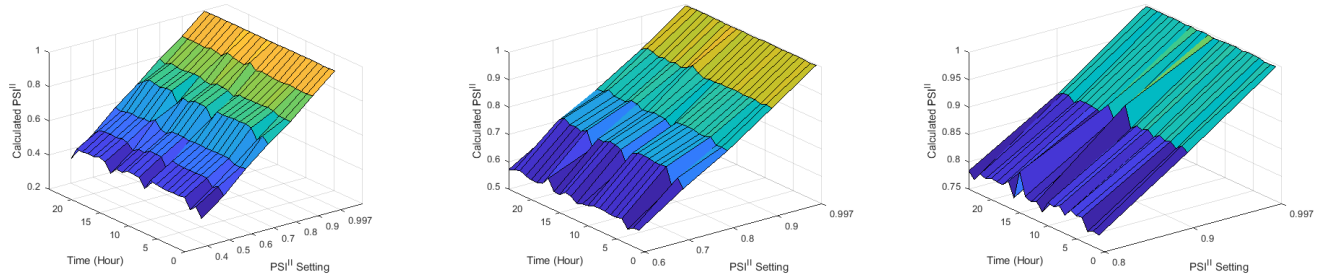

(a) $\mathrm{PSI}^{\mathrm{I,req}} = 0.4$ (b) $\mathrm{PSI}^{\mathrm{I,req}} = 0.6$ (c) $\mathrm{PSI}^{\mathrm{I,req}} = 0.8$

Fig. 2: Comparison of calculated $\mathrm{PSI}^{\mathrm{II}}$ under different $\mathrm{PSI}^{\mathrm{I}}$ and $\mathrm{PSI}^{\mathrm{II}}$ settings

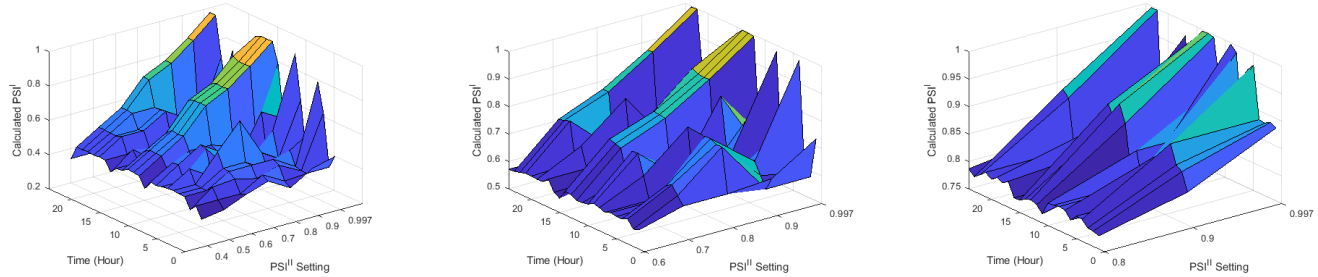

(a) $\mathrm{PSI}^{\mathrm{I,req}} = 0.4$ (b) $\mathrm{PSI}^{\mathrm{I,req}} = 0.6$ (c) $\mathrm{PSI}^{\mathrm{I,req}} = 0.8$

Fig. 3: Comparison of calculated $\mathrm{PSI}^{\mathrm{I}}$ under different $\mathrm{PSI}^{\mathrm{I}}$ and $\mathrm{PSI}^{\mathrm{II}}$ settings

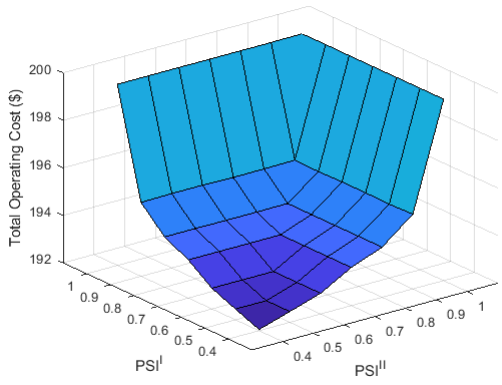

Fig. 4: Comparison of total operating cost under different $\mathrm{PSI}^{\mathrm{I}}$ and $\mathrm{PSI}^{\mathrm{II}}$ settings

of $\mathrm{PSI}^{\mathrm{I,req}}$ or $\mathrm{PSI}^{\mathrm{II,req}}$ will require a significant increase of cost when $\mathrm{PSI}^{\mathrm{I,req}}$ or $\mathrm{PSI}^{\mathrm{II,req}}$ is greater than 0.9.

IV. Conclusions

In this paper, we proposed a new resilient microgrid scheduling model that explicitly guarantees the resiliency requirements of loads with multi-level priorities. For each priority level, the resiliency requirement of load is enforced by a chance constraint. Numerical simulations validated the effectiveness and accuracy of the proposed resilient microgrid scheduling model. The impacts of resiliency requirement of loads with high priority on the resiliency of loads with low priority are analyzed as well.

References

[1] CERTS Microgrid Concept, 2003, [Online]. Available: http://certs.lbl.gov/certs-der-micro.html.

[2] D. E. Olivares et al., "Trends in microgrid control," *IEEE Trans. Smart Grid*, vol. 5, no. 4, pp. 1905-1919, Jul. 2014.

[3] A. Hussain, V. Bui and H. Kim, "Resilience-oriented optimal operation of networked hybrid microgrids," *IEEE Trans. Smart Grid*, vol. 10, no. 1, pp. 204-215, Jan. 2019.

[4] A. Hirsch, Y. Parag and J. Guerrero, "Microgrids: A review of technologies, key drivers, and outstanding issues," *Renew. Sustain. Energy Rev.*, vol. 90, pp. 402-411, Jul 2018.

[5] A. G. Tsikalakis and N. D. Hatziargyriou, "Operation of microgrids with demand side bidding and continuity of supply for critical loads," *Eur. Trans. Electr. Power*, vol. 21, no. 2, pp. 1238–1254, Mar. 2011.

[6] B. Zhao, Y. Shi, X. Dong, W. Luan, and J. Bornemann, "Short-Term Operation Scheduling in Renewable-Powered Microgrids: A Duality-Based Approach," *IEEE Trans. Sustain. Energy*, vol. 5, no. 1, pp. 209-217, Jan. 2014.

[7] M. Q. Wang, and H. B. Gooi, "Spinning Reserve Estimation in Microgrids," *IEEE Trans. Power Syst.*,, vol.26, no.3, pp.1164-1174, Aug. 2011.

[8] G. Liu, M. Starke, B. Xiao, X. Zhang and K. Tomsovic, "Microgrid Optimal Scheduling With Chance-Constrained Islanding Capability," *Electr. Power Syst. Res.*, vol. 145, pp. 197-206, Feb. 2017,

[9] G. Liu, M. Starke, B. Xiao, and K. Tomsovic, "Robust Optimization Based Microgrid Scheduling with Islanding Constraints," *IET Gen. Trans. & Distri.*, vol. 11, no. 7, pp. 1820-1828, May 2017.

[10] A. Khodaei, "Microgrid Optimal Scheduling With Multi-Period Islanding Constraints," *IEEE Trans. Power Syst.*, vol. 29, no. 3, pp. 1383-1392, May 2014.

[11] A. Khodaei, "Resiliency-Oriented Microgrid Optimal Scheduling ," *IEEE Trans. Smart Grid*, vol. 5, no. 4, pp. 1584-1591, Jul. 2014.